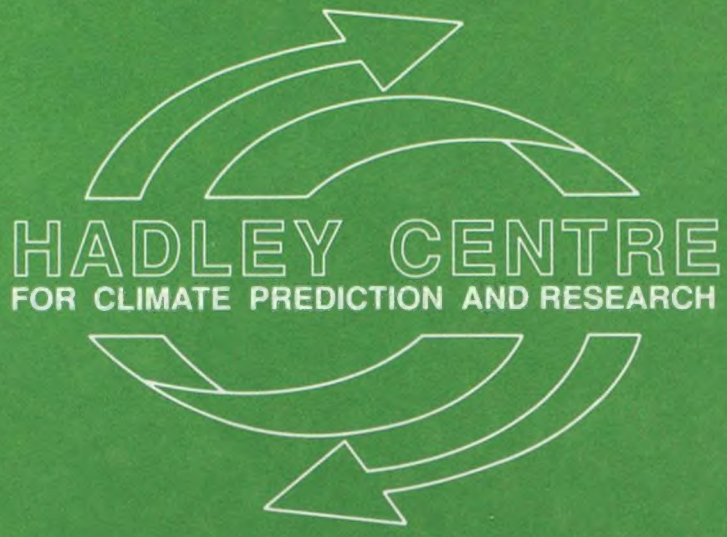

Simulation of the Tropical Diurnal Cycle in a Climate Model

by

D. P. Rowell

CRTN 3

October 1990

CLIMATE
RESEARCH
TECHNICAL
NOTE

Hadley Centre
Meteorological Office
London Road
Bracknell
Berkshire RG12 2SY

CLIMATE RESEARCH TECHNICAL NOTE NO. 3

SIMULATION OF THE TROPICAL DIURNAL CYCLE IN A CLIMATE MODEL

by

D P ROWELL

Hadley Centre for Climate Prediction and Research
Meteorological Office
London Road
Bracknell
Berkshire RG12 2SY
U. K.

NOTE: This paper has not been published. Permission to quote from it should be obtained from the Director of the Hadley Centre.

Abstract

The diurnal cycle of an 11-layer high resolution climate model is investigated using data extracted every 6 hours from a 30-day simulation. Emphasis is placed mainly on the North African summer. The diurnal cycle of precipitation has large realistic amplitude, but its phase is misplaced by about 6 hours due to the model's inability to represent some important mesoscale processes. In turn, the cycle of convective activity has a substantial impact on model dynamics, particularly on the divergent flow, and to a lesser extent on the total flow. This is illustrated by maps of upper and lower tropospheric divergence, surface temperature and evaporation, and by latitude cross-sections of zonal and meridional wind, temperature, humidity, and the Hadley circulation. Globally, the amplitude of diurnal variability (illustrated by a number of variables) is greatest over major tropical land masses, but is also significant over tropical oceanic regions and some mid-latitude continental regions.

It is concluded that despite some problems in the simulation of diurnal variability, this is an important aspect of the model's performance, and needs to be well understood. This is particularly so for the appropriate analysis of the time-mean flow, which can only be correctly interpreted when computed from sub-daily sampling of the model evolution.

1) Introduction

The ability of general circulation models (GCMs) to simulate the diurnal cycle is a subject that has received little attention to date. It is not however an issue that can be ignored when analyzing model diagnostics, particularly for studies concerned with the flow and variability of the tropical atmosphere. The earliest published investigations of the simulation of diurnal variability with a sophisticated GCM were those of Zwiers and Hamilton (1986), who looked at two 60-day integrations of the Canadian Climate Centre GCM, and that of Wilson and Mitchell (1986) who performed a sensitivity experiment changing the resolution of the diurnal cycle of cloud and radiative fluxes. Slingo et al. (1987) briefly describe a 30-day simulation of the diurnal variability of outgoing long-wave radiation, and finally Hsu and Hoskins (1989) have considered in detail the diurnal and semi-diurnal cycles in the ECMWF analyses. The studies of both Zwiers and Hamilton and of Hsu and Hoskins found the geographical dependence of both the amplitude and phase of diurnal variability to be broadly similar to available observational studies (eg: Hastenrath, 1972, Wallace and Tadd, 1974), although some serious limitations were noted, particularly in the stratosphere and upper troposphere due to the presence of a "rigid-lid" upper boundary condition.

The motivation behind the present study was the realisation that diagnostics of all model variables must be produced as a mean over a number of points within the diurnal cycle, and that to sample only once every 24 hours is liable to produce misleading results, particularly when studying the tropical atmosphere. This was first noted at the Meteorological Office by Cunnington and Rowntree (1986), but appears to have received little recognition since. A more detailed study is presented here, focusing mainly upon the North African summer. This region presents a large mass of land to the tropical atmosphere, and thus experiences substantial diurnal variability, allowing the study of potentially large changes between nighttime and daytime circulations.

2) The Model and Experimental Method

The GCM used is the "third annual cycle" version of the Meteorological Office climate model, which has 11 levels in the vertical, and a horizontal resolution here of 2.5^0 latitude by 3.75^0 longitude. The representation of physical processes is described by Cunnington and Rowntree (1986). Of particular importance to this study is the radiation scheme. A full calculation is performed every 3 hours, with radiative increments added to the temperature fields at every time-step (10 minutes). The scheme is fully interactive with water vapour, but clouds however are prescribed with zonally-meaned amounts and height with only seasonal variation. This may have the effect of reducing the amplitude of diurnal variability, since the interaction of cloud and radiation are thought to play an important role in the diurnal cycle (Gray and Jacobson, 1977). Also of importance to tropical diurnal variability is the convection scheme. This is based upon the parcel theory and models an ensemble of convective plumes which are modified by entrainment and detrainment of the environmental air. The initiation, depth and intensity of convection is thus wholly dependent upon the grid point moisture and temperature profiles.

The results described in the following sections are taken from part of a 210-day integration running from the end of March to the end of October, forced by observed sea surface temperatures for 1988, updated every 5 days. 1988 was a year of approximately average rainfall throughout Sub-Saharan North Africa, both in the model simulation and observed data. For 30 days of the integration, from August 1 to 30, variables at all levels were kept every 6 hours. All data are instantaneous values, apart from rainfall, snowfall, evaporation, sensible heat

flux and radiative heat fluxes which are each accumulated over the 6 hour periods. The results displayed are means over this 30-day period, computed separately for 0600, 1200, 1800 and 2400 GMT.

Although many of the diagrams are discussed only very briefly, they are all included for those readers wishing to study them in more detail.

3) Results

a) Precipitation

Fig.1 shows the modelled diurnal cycle of precipitation (convective + large scale) over northern and central Africa, and also the mean over the entire 24 hour period. A marked maximum occurs between 0600 and 1800 GMT over the North African land mass. It is noticeable that largest rainfall values occur to the east of the Greenwich meridian between 0600 and 1200, where solar heating is larger during this period, and similarly the 1200-1800 maximum occurs to the west of the meridian. This close link between the local diurnal cycle of precipitation and the local diurnal solar cycle is easily explained: Short wave radiative heating rapidly warms the land surface after sunrise (Fig.2), until the lowest layers of the model atmosphere become sufficiently unstable to initiate convection. Instability is further aided by the increasing moisture content of the boundary layer through evaporation (Fig.3). The model's development of convective activity is then further enhanced by a positive feedback cycle which acts through latent heating increasing convergence, particularly at low levels where a continued and enhanced supply of moisture maintains an unstable profile. Later, as the land surface cools, the lower troposphere regains stability, and convective activity ceases (or is much reduced). The phase of this cycle is however in disagreement with observational studies (McGarry and Reed, 1978; Reed and Jaffe, 1981; Duvel, 1989) which show convective activity in Sub-Saharan West Africa does not peak until the late evening (or later still in some areas). This delay occurs because the majority of precipitation in the region is provided by relatively long-lived squall lines, which generate during the afternoon soon after the peak in solar heating (eg: Aspliden et al., 1976; Martin and Schreiner, 1981), but often take several hours to reach their maximum size and intensity, with much of their growth resulting from the effects of mesoscale feedbacks (Zipser, 1977). Squall lines clearly exist on scales far too small to be resolved by a global model, and so their impact on the phase of the diurnal cycle is not incorporated.

b) The Divergent Flow

The model's dynamical fields are produced as instantaneous values, and it is the daily evolution of these that is of primary interest. The dynamics interacts strongly with precipitation since the convection scheme is both driven by and drives the regional circulation, particularly its divergent component.

Perhaps the most important feature of the tropical atmosphere is the Hadley circulation. The modelled diurnal cycle of this over the African sector is illustrated in Fig.4. At 1200 and 1800 GMT the well known double cell structure is seen, with strong ascent at the ITCZ over the Sahel and Soudan areas (where maximum precipitation is seen, Fig.1), with descending arms to the north and south. However, after the sun sets, and convective activity largely ceases, this large scale Hadley circulation alters substantially. The ascent over the Sahel/Soudan areas is substantially reduced and moves north over the warmer desert surface. In response the compensating subsidence to the south is considerably weakened and occupies only a limited range of latitudes. This allows an area of weak ascent to develop further south, over the warmer surface of central Africa and the mountainous regions of equatorial East Africa, with compensating subsidence to the south. Thus a double cell structure is formed. The picture

seen at 0600 GMT is probably during the transition between the nighttime and daytime circulations.

Figs.5 and 6 show the diurnal variability of the spatial distribution of divergence in the upper and lower troposphere. The daytime pattern seen in these diagrams is closely linked to that described for precipitation, whereas the nighttime pattern is related more to the surface temperature distribution.

c) The Total Flow

The impact of the daily cycle of solar heating on the total flow, including its rotational component, is now illustrated. Latitude cross-sections of the African sector are used to describe the variability of zonal and meridional wind, temperature, and humidity (Figs.7 to 12).

Diurnal variability of the wind fields (Figs.7 to 9) are greatest in the lower and upper troposphere, this being due to the large diurnal cycle of convective activity modulating the inflow to convective plumes in the boundary layer, and their outflow in the upper troposphere. In the lower troposphere anomalous vertical shear of the zonal flow (Fig.7) is at least in part a response to variability in the temperature field (Fig.10). Upper level zonal anomalies are of less significance, since the mean flow there is larger. Diurnal variability of the meridional flow (Figs.8 and 9) is slightly larger than that of the zonal flow, and is certainly more significant, with a similar amplitude to the mean flow. Near the surface, variability in the penetration of southerly flow into the fringes of the Sahara is closely linked to the changes in low level convergence and the Hadley circulation.

The diurnal cycle of the temperature profile (Fig.10) clearly shows the changes in boundary layer stability discussed above, and also changes in mid-tropospheric heating due to latent heat release (around 10 to 15°N). The daytime humidity profiles (Figs.11 and 12) show a deficit of moisture in the boundary layer and through much of the troposphere due to the sink provided by convective rainfall. At 1800 GMT (when the convective sink is small) a positive anomaly (in relative humidity) occurs in the upper troposphere due to the continued large scale ascent of the Hadley circulation which is pumping moisture from the boundary layer up to higher levels.

d) A Global View

The discussion so far has been concerned solely with the modelled diurnal cycle over northern and central Africa. Although broadly speaking the majority of these results may also apply to other tropical continental regions, it is instructive to look briefly at diurnal variability on a global scale. Fig.13 shows the amplitude of the modelled diurnal cycle of precipitation in August, relative to mean precipitation. As might be intuitively expected, and as shown by observations (eg: Meisner and Arkin, 1987; Duvel, 1989), diurnal variability is far greater over the land than over oceans because the much larger heat capacity of the later responds little to the daily cycle of solar heating (indeed, model sea temperatures are fixed through the day). Also the northern hemisphere generally shows greater variability than the southern hemisphere, since in the latter the winter or dry seasons are simulated. Tropical regions are subject to a larger daily cycle of precipitation than mid-latitudes, since the diurnal variability of radiative forcing is of larger amplitude in the tropics, and because convective rainfall is far more sensitive to the diurnal cycle of surface heat fluxes than is large scale precipitation. Some continental mid-latitude regions do however demonstrate large diurnal variability.

Fig.14 shows the diurnal variability of the zonally meaned Hadley circulation. Even though each diagram is a mean of both daytime and nighttime values, large variations in the magnitude of ascent and descent still occur. The main effect however is probably from the Asian and African land masses, whose local solar

times differ by only about six hours. The Walker circulation in the northern tropics is illustrated in Fig.15, and substantial variability occurs not only in the intensity of individual cells, but also in the pattern of the entire circulation. The Asian and African land masses are again most affected, but the impact on all longitudes is significant.

Finally, the modelled diurnal cycle of velocity potential is illustrated in Fig.16. Major differences occur between nighttime and daytime patterns over Africa (compare also with Fig.6) and over the tropical Atlantic. There is also much diurnal variability in the intensity and position of the minimum over Southeast Asia, with increased divergent outflow during the day (here local solar time is 6 to 9 hours ahead of GMT). Lesser variability is also seen throughout the remainder of the tropics.

4) Concluding Remarks

Available observational studies of the geographical and height dependence of the diurnal cycle are inevitably limited by a paucity of frequent radiosonde ascents, and validation of the detailed results from a GCM integration is therefore almost impossible. Particular problems may arise, however, due to the model's limited vertical resolution (Hsu and Hoskins, 1989), and as shown here due to the model's inability to simulate mesoscale and convective weather systems and their impact on their environment. A further problem, particular to this model, is its fixed rather than interactive representation of cloud distribution, and this may further weaken the quality of the model's simulation of diurnal variability.

The starting point of this investigation was to study the magnitude of diurnal variability in the atmospheric dynamics simulated by a GCM, and to determine which model diagnostics should be sampled on a sub-daily time scale to avoid obtaining biased results. The effect of the daily solar cycle on the model's flow, in particular the divergent component, has been shown to be substantial. Whether or not the detailed circulation changes through the day are well simulated, it is essential to recognise the impact of the diurnal cycle on the model dynamics, and where possible diagnostics should be meaned over sub-daily samples of model output.

Acknowledgements

I am grateful to Dr. John Owen for his extensive assistance in running the model, and to Chris Folland for comments on the script.

References

Aspliden, C.I., Tourre, Y. and Sabine, J.B. 1976 Some climatological aspects of West African disturbance lines during GATE. Mon. Wea. Rev., 104, 1029-1035

Cunnington, W.M. and Rowntree, P.R. 1986 Simulation of the Saharan atmosphere - dependence on moisture and albedo. Q. J. R. Meteorol. Soc., 112, 971-999

Duvel, J.P. 1989 Convection over tropical Africa and the Atlantic ocean during northern summer. Part I: Interannual and diurnal variations. Mon. Wea. Rev., 117, 2782-2799

Gray, W.M. and Jacobson, R.W. 1977 Diurnal variation of deep cumulus convection. Mon. Wea. Rev., 105, 1171-1188

Hastenrath, S. 1972 Daily wind, pressure and temperature variation up to 30km over the tropical western Pacific. Q. J. R. Meteorol. Soc., 98, 48-59

Hsu, H.-H. and Hoskins, B.J. 1989 Tidal fluctuations as seen in ECMWF data. Q. J. R. Meteorol. Soc., 115, 247-264

McGarry, M.M. and Reed, R.J. 1978 Diurnal variation in convective activity and precipitation during phases II and III of GATE. Mon. Wea. Rev., 106, 101-113

Martin,D.W., and A.J.Schreiner, 1981: Characteristics of West African and East Atlantic cloud clusters: A survey from GATE. Mon. Wea. Rev., 109, 1671-1688.

Meisner, B.N. and Arkin, P.A. 1987 Spatial and annual variations in the diurnal cycle of large-scale tropical convective cloudiness and precipitation. Mon. Wea. Rev., 115, 2009-2032

Reed, R.J. and Jaffe, K.D. 1981 Diurnal variation of summer convection over west Africa and tropical eastern Atlantic during 1974 and 1978. Mon. Wea. Rev., 109, 2527-2534

Slingo, A., Wilderspin, R.C. and Brentnall, S.J. 1987 Simulation of the diurnal cycle of outgoing long-wave radiation with an atmospheric GCM. Mon. Wea. Rev., 115, 1451-1457

Wallace, J.M. and Tadd,R.F. 1974 Some further results concerning the vertical structure of atmospheric tidal motions within the lowest 30 kilometers. Mon. Wea. Rev., 102, 795-803

Wilson, C.A. and Mitchell, J.F.B. 1986 Diurnal variation and cloud in a general circulation model. Q. J. R. Meteorol. Soc., 112, 347-369

Zipser,E.J. 1977 Mesoscale and convective-scale downdrafts as distinct components of squall-line structure. Mon. Wea. Rev., 105, 1568-1589

Zwiers, F. and Hamilton, K. 1986 Simulation of solar tides in the Canadian Climate Centre general circulation model. J. Geophys. Res., 91, 11877-11896

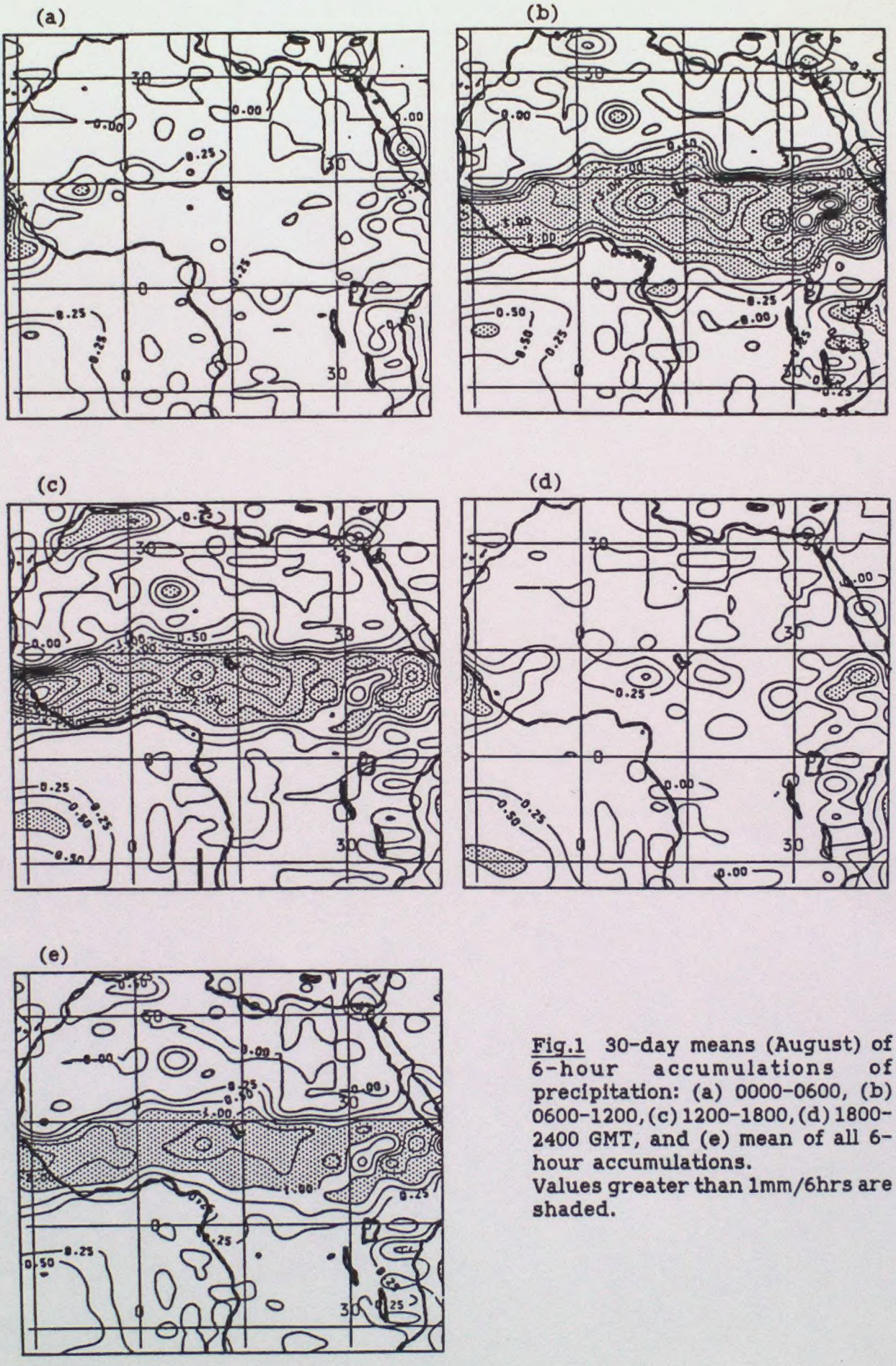

Fig.1 30-day means (August) of 6-hour accumulations of precipitation: (a) 0000-0600, (b) 0600-1200, (c) 1200-1800, (d) 1800-2400 GMT, and (e) mean of all 6-hour accumulations.
Values greater than 1mm/6hrs are shaded.

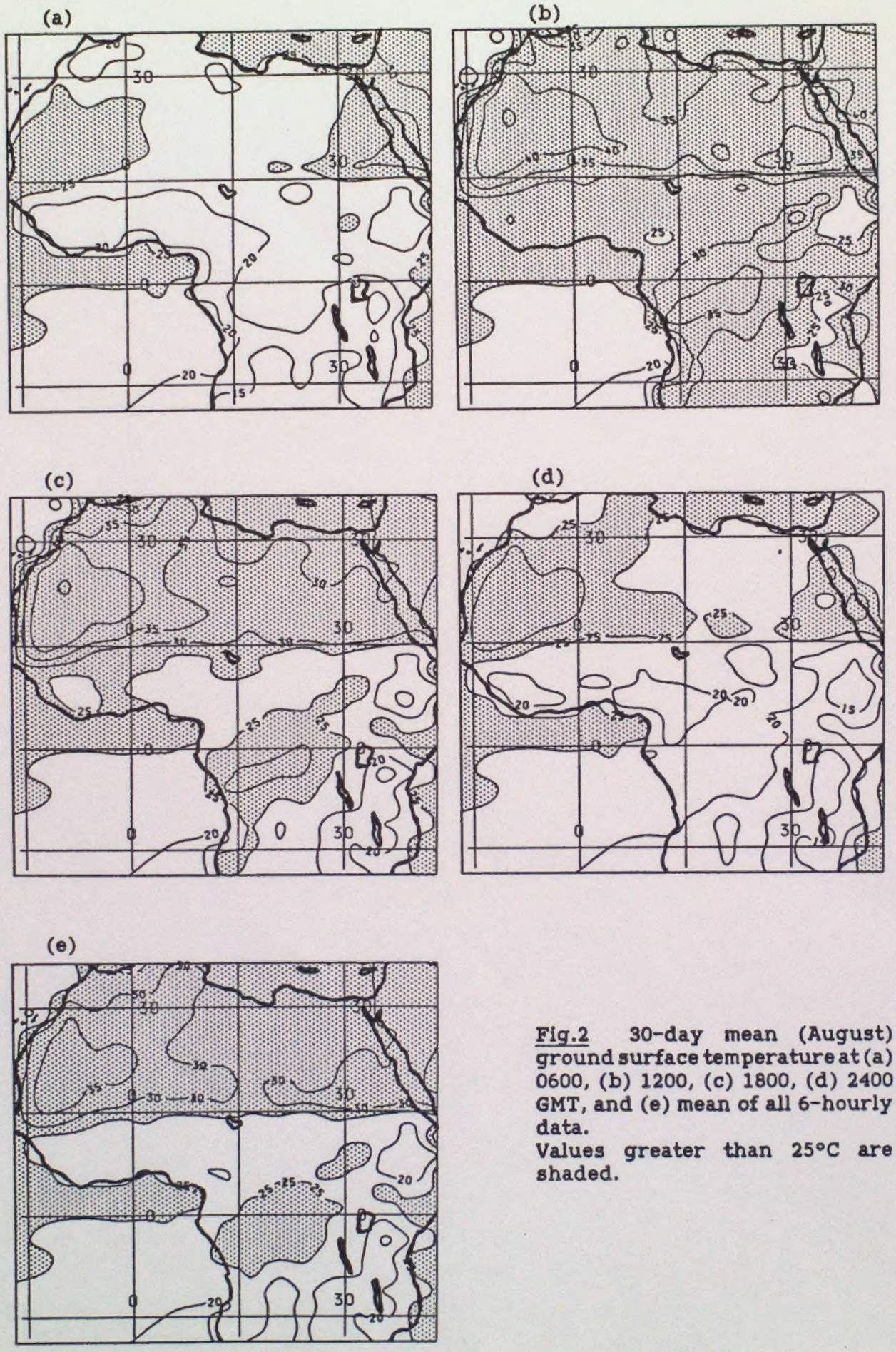

Fig.2 30-day mean (August) ground surface temperature at (a) 0600, (b) 1200, (c) 1800, (d) 2400 GMT, and (e) mean of all 6-hourly data.
Values greater than 25°C are shaded.

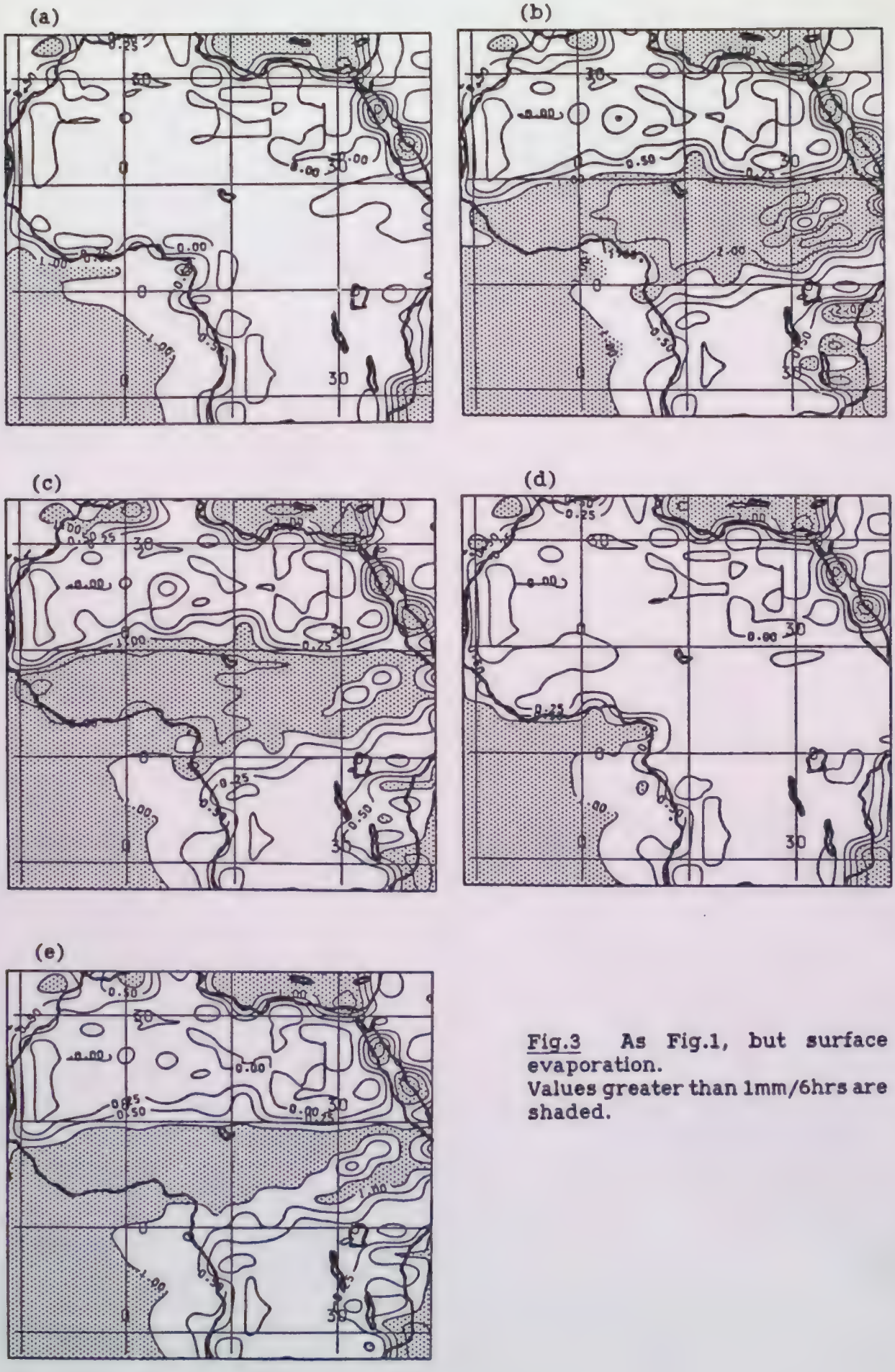

Fig.3 As Fig.1, but surface evaporation.
Values greater than 1mm/6hrs are shaded.

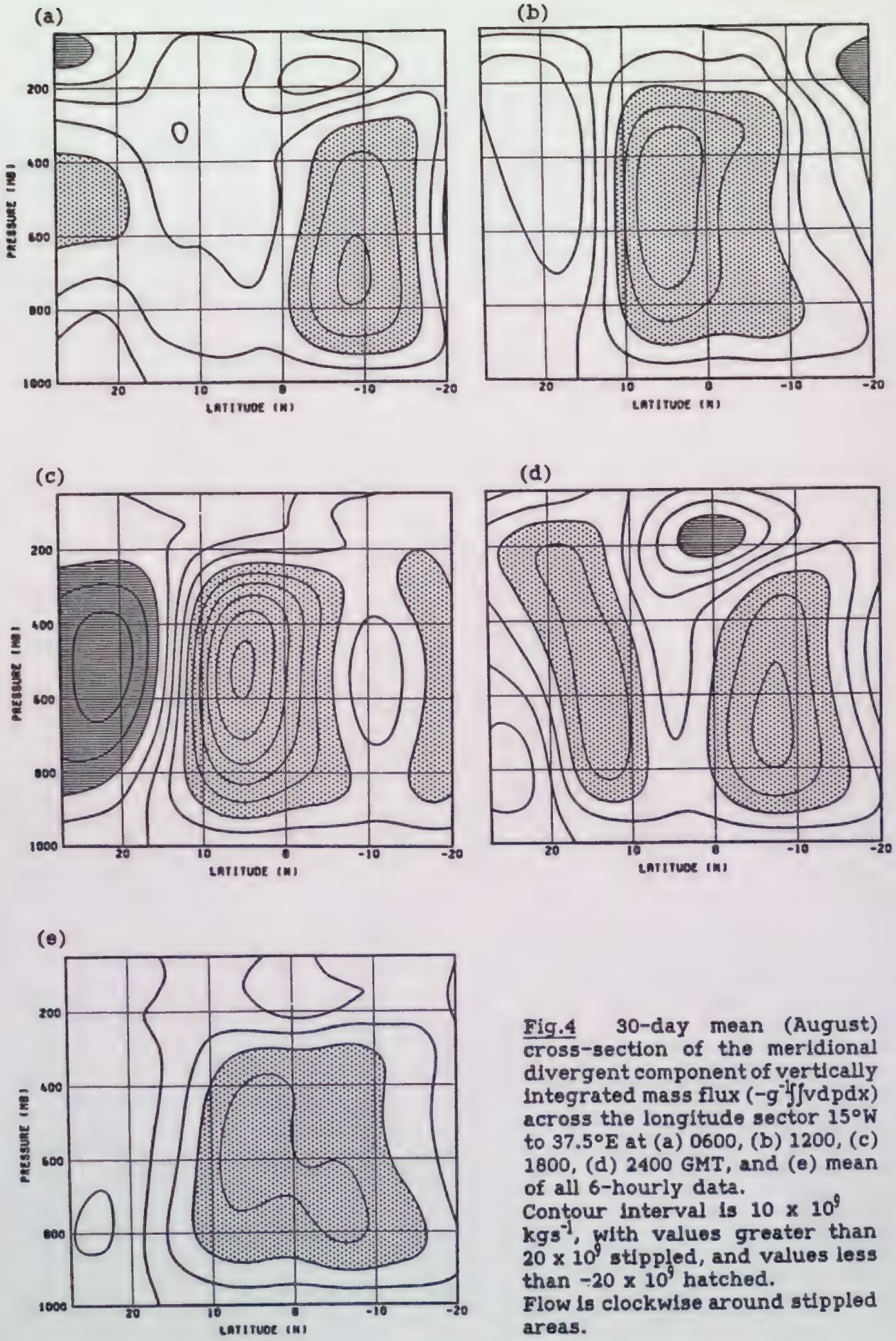

Fig.4 30-day mean (August) cross-section of the meridional divergent component of vertically integrated mass flux ($-g^{-1}\int\int vdpdx$) across the longitude sector 15°W to 37.5°E at (a) 0600, (b) 1200, (c) 1800, (d) 2400 GMT, and (e) mean of all 6-hourly data.
Contour interval is 10×10^9 kgs^{-1}, with values greater than 20×10^9 stippled, and values less than -20×10^9 hatched.
Flow is clockwise around stippled areas.

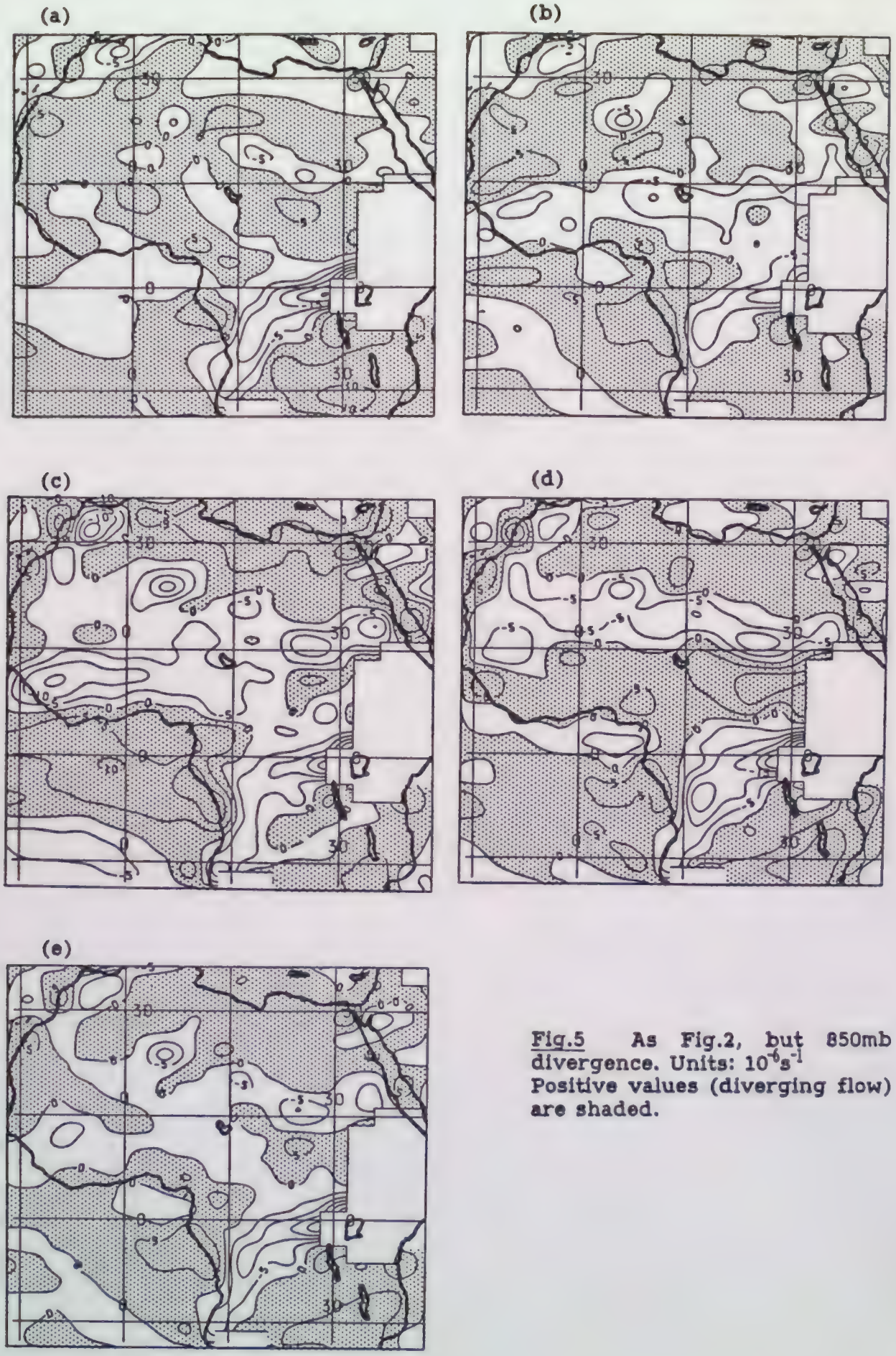

Fig.5 As Fig.2, but 850mb divergence. Units: $10^{-6}s^{-1}$
Positive values (diverging flow) are shaded.

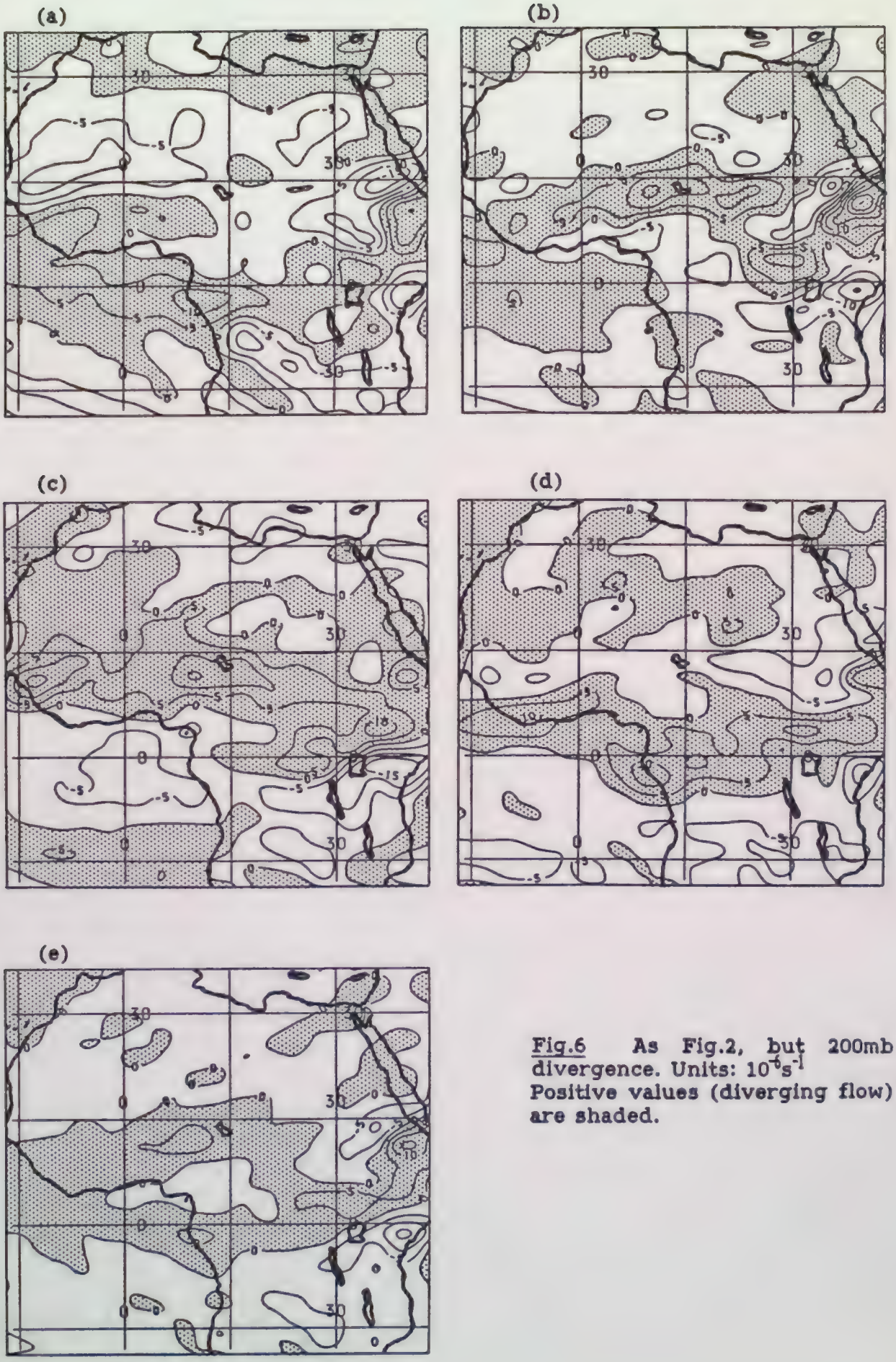

Fig.6 As Fig.2, but 200mb divergence. Units: $10^{-6}s^{-1}$
Positive values (diverging flow) are shaded.

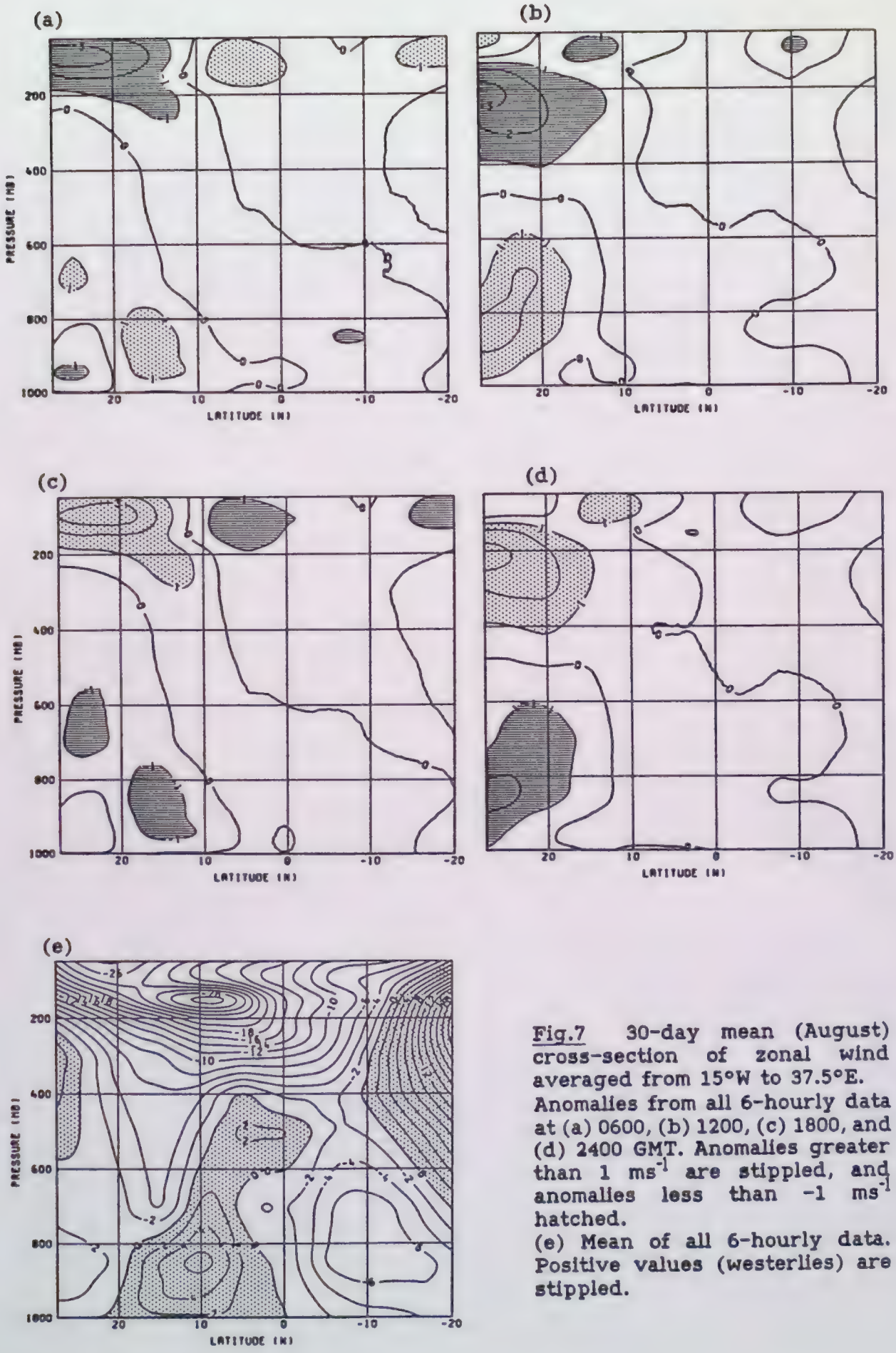

Fig.7 30-day mean (August) cross-section of zonal wind averaged from 15°W to 37.5°E. Anomalies from all 6-hourly data at (a) 0600, (b) 1200, (c) 1800, and (d) 2400 GMT. Anomalies greater than 1 ms^{-1} are stippled, and anomalies less than -1 ms^{-1} hatched.
(e) Mean of all 6-hourly data. Positive values (westerlies) are stippled.

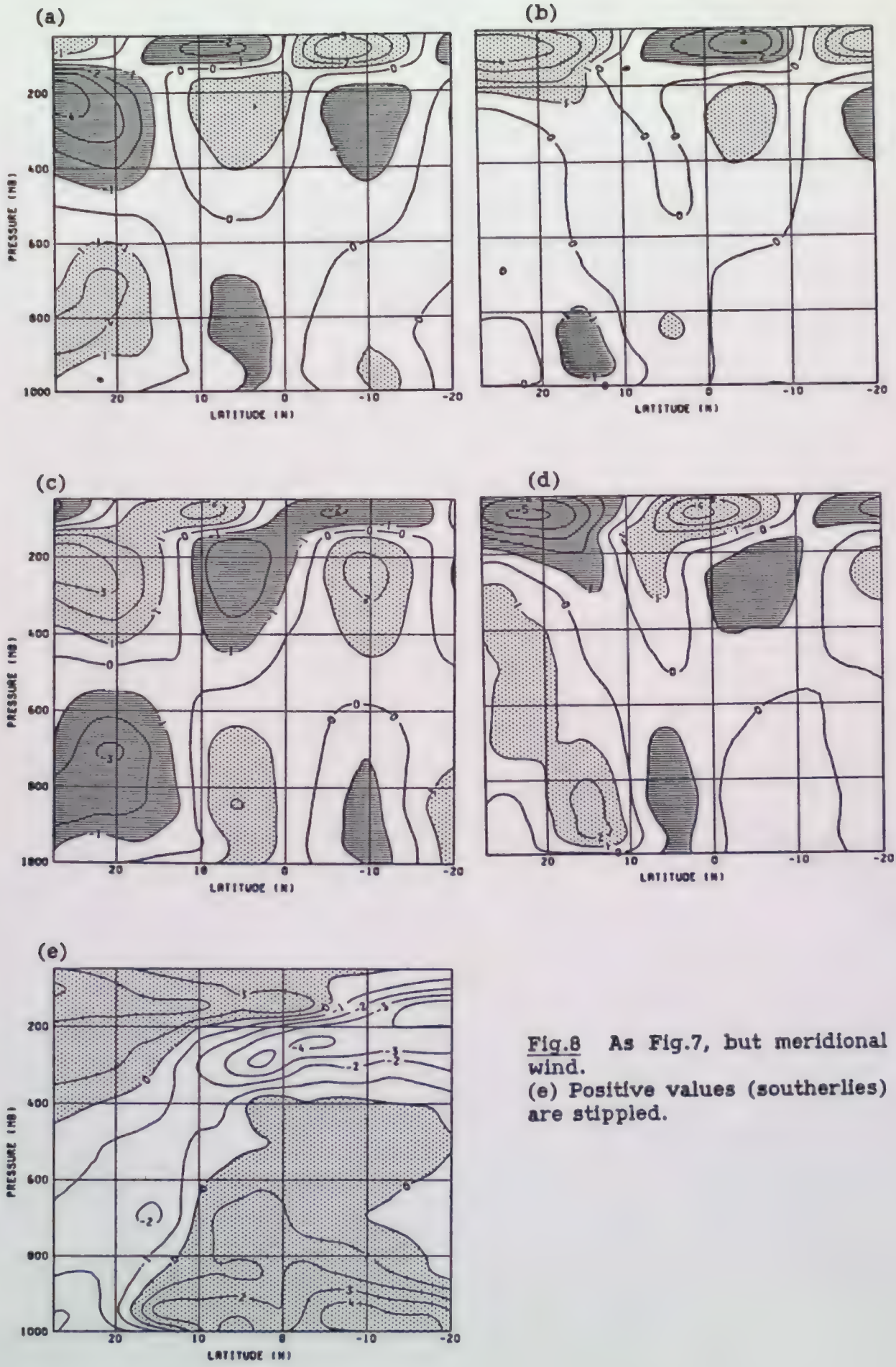

Fig.8 As Fig.7, but meridional wind.
(e) Positive values (southerlies) are stippled.

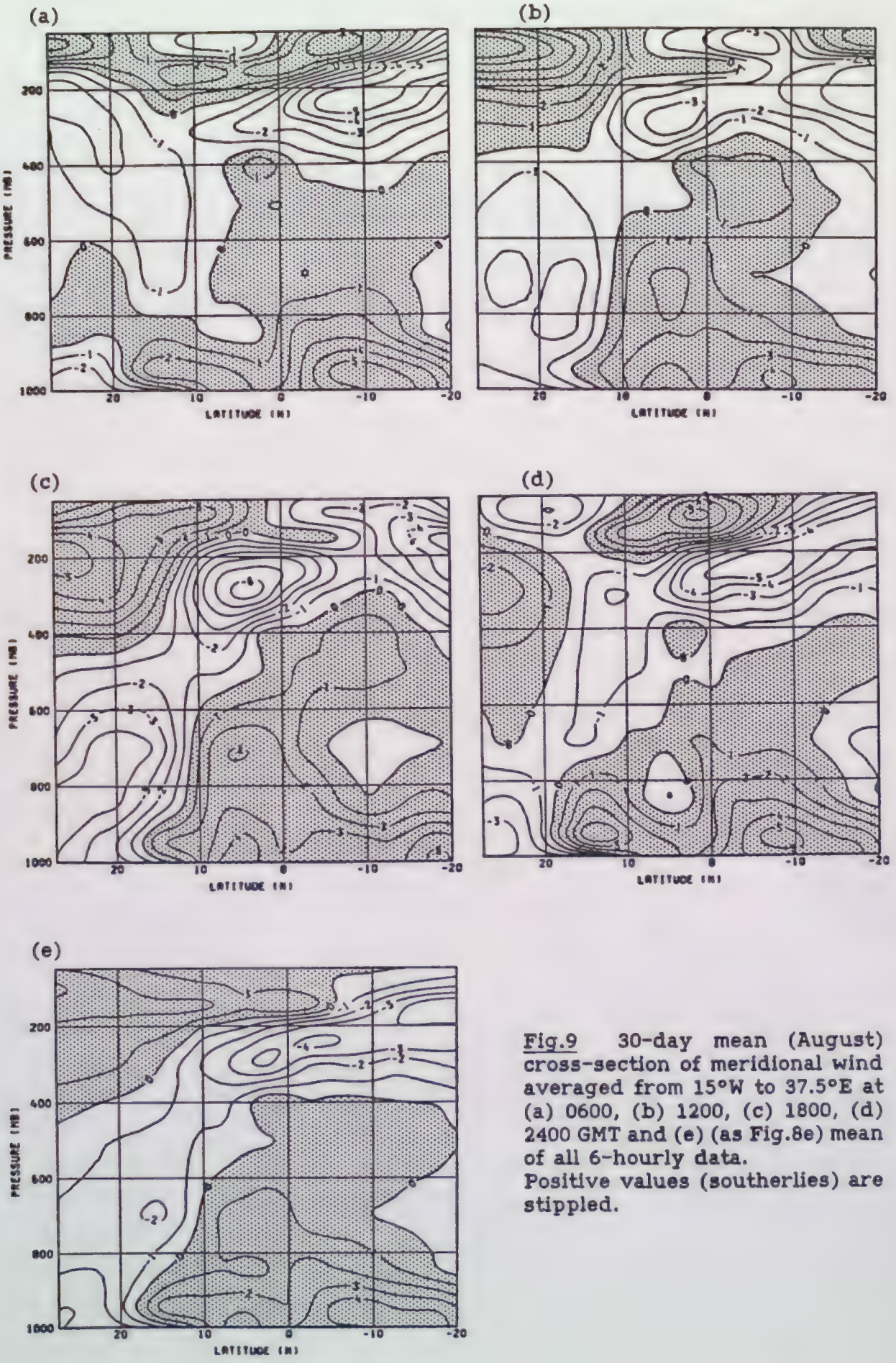

Fig.9 30-day mean (August) cross-section of meridional wind averaged from 15°W to 37.5°E at (a) 0600, (b) 1200, (c) 1800, (d) 2400 GMT and (e) (as Fig.8e) mean of all 6-hourly data.
Positive values (southerlies) are stippled.

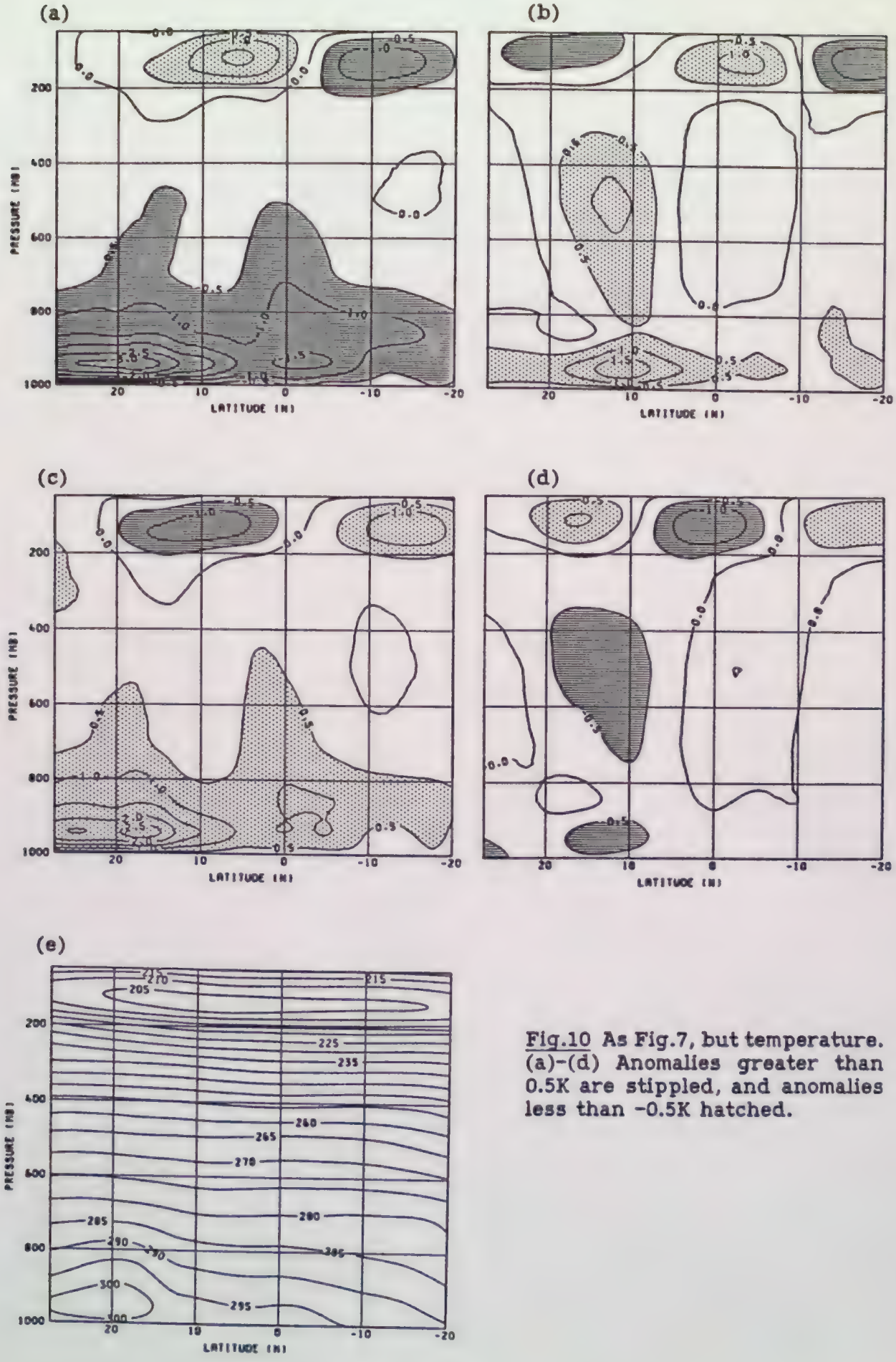

Fig.10 As Fig.7, but temperature. (a)-(d) Anomalies greater than 0.5K are stippled, and anomalies less than -0.5K hatched.

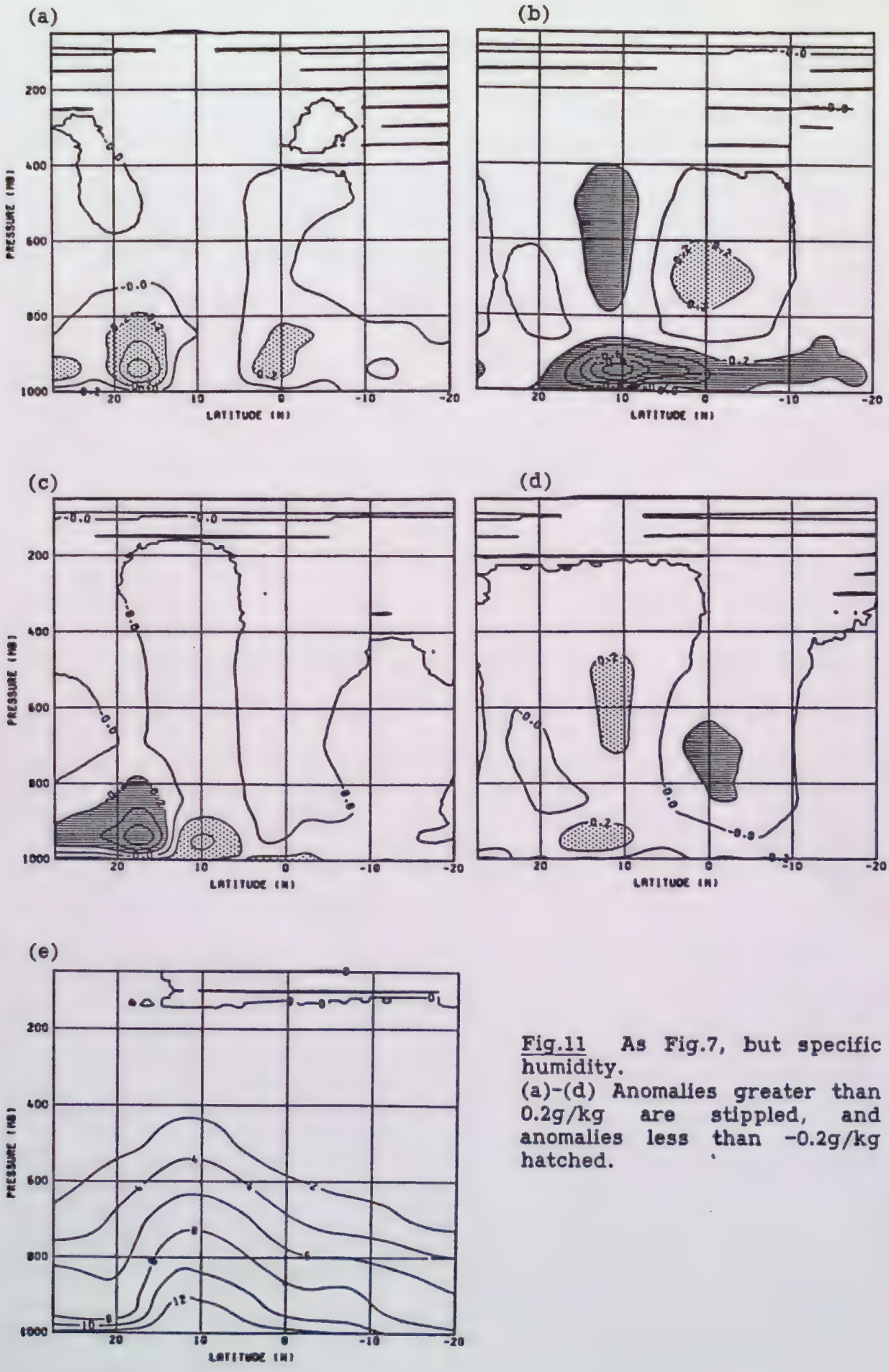

Fig.11 As Fig.7, but specific humidity.
(a)-(d) Anomalies greater than 0.2g/kg are stippled, and anomalies less than -0.2g/kg hatched.

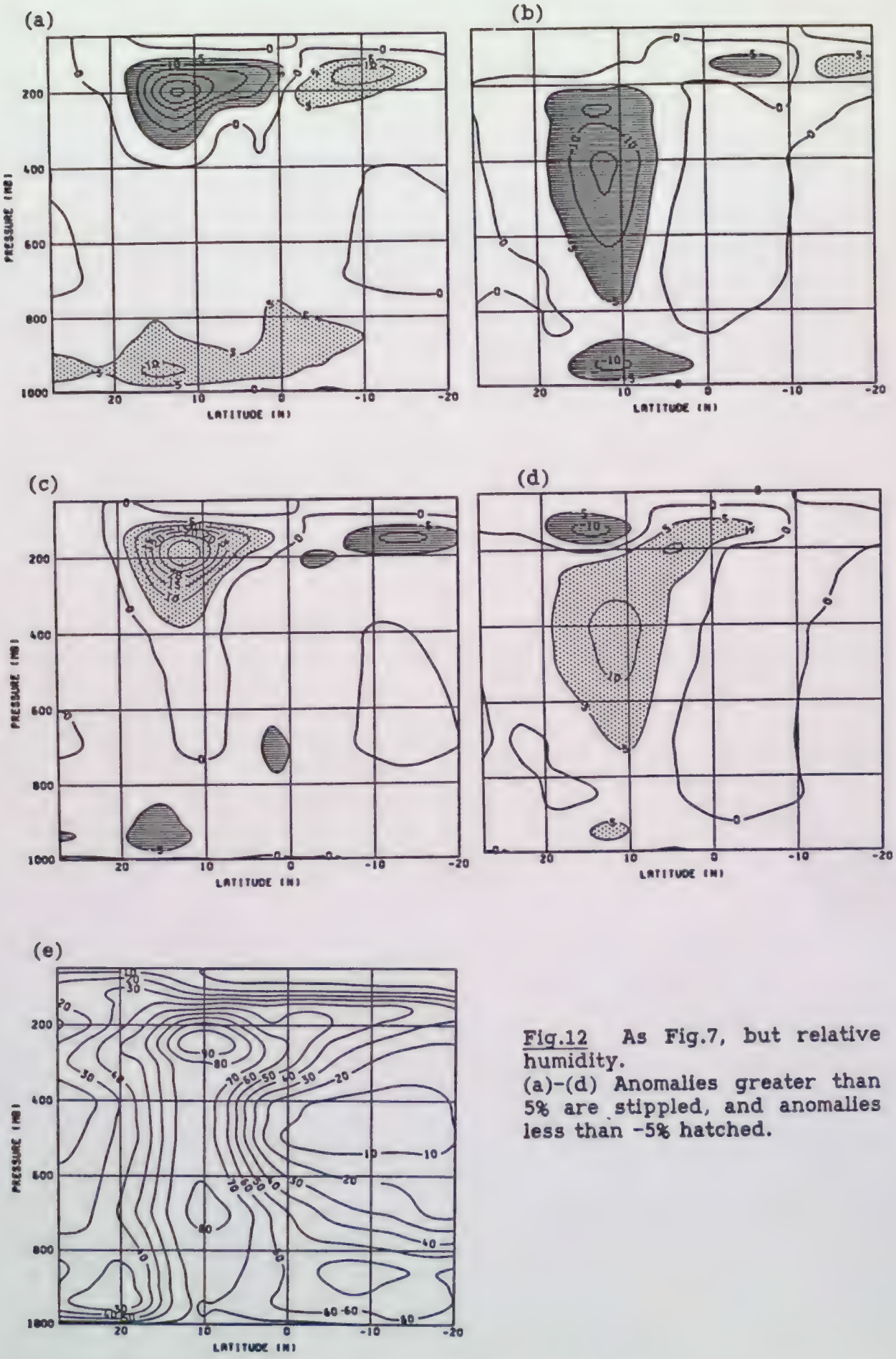

Fig.12 As Fig.7, but relative humidity.
(a)-(d) Anomalies greater than 5% are stippled, and anomalies less than -5% hatched.

(a)

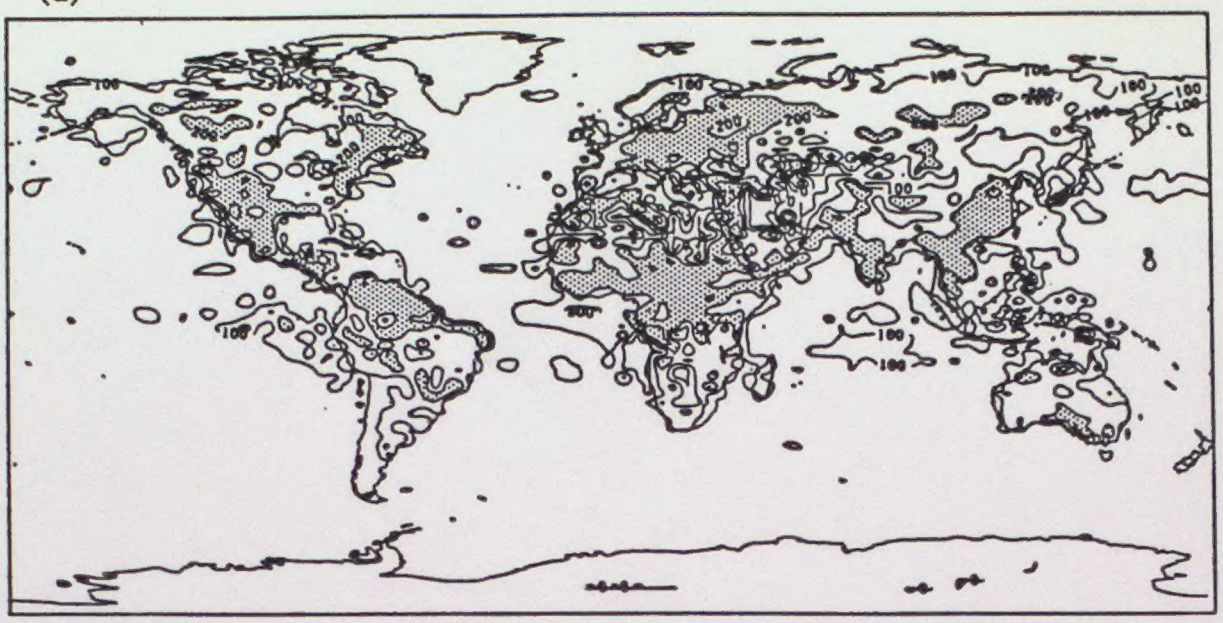

(b)

Fig.13 (a) Amplitude of the diurnal variability of August precipitation (at each grid point maximum minus minimum of the 30-day means of 0000-0600, 0600-1200, 1200-1800, and 1800-2400 GMT 6-hour accumulations), scaled by the mean 6-hourly precipitation. Values greater than 200% are shaded.
(b) 30-day accumulated precipitation. Values greater than 5mm/day are shaded.

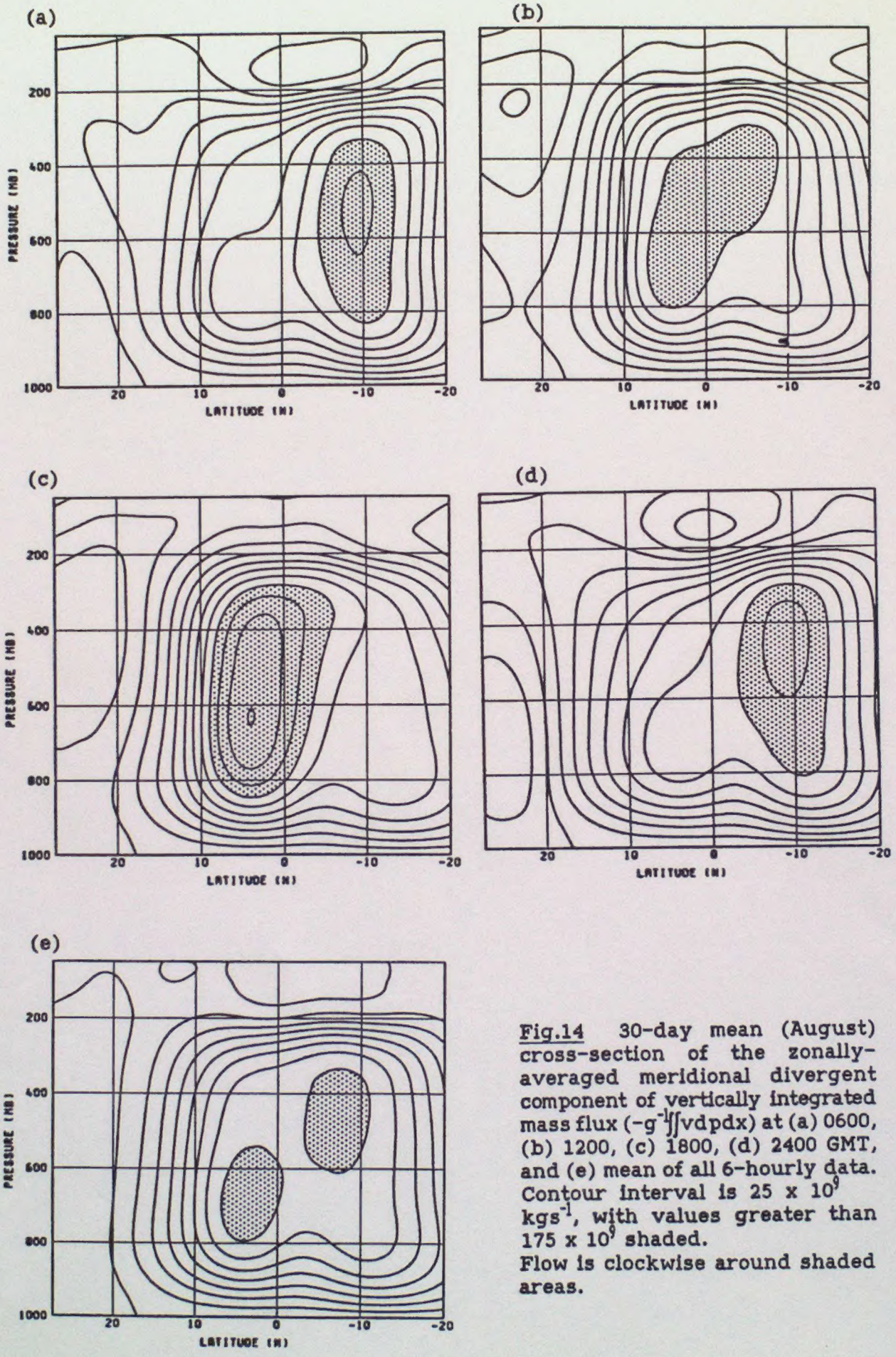

Fig.14 30-day mean (August) cross-section of the zonally-averaged meridional divergent component of vertically integrated mass flux ($-g^{-1}\int\int vdpdx$) at (a) 0600, (b) 1200, (c) 1800, (d) 2400 GMT, and (e) mean of all 6-hourly data. Contour interval is 25 x 10^9 kgs^{-1}, with values greater than 175 x 10^9 shaded.
Flow is clockwise around shaded areas.

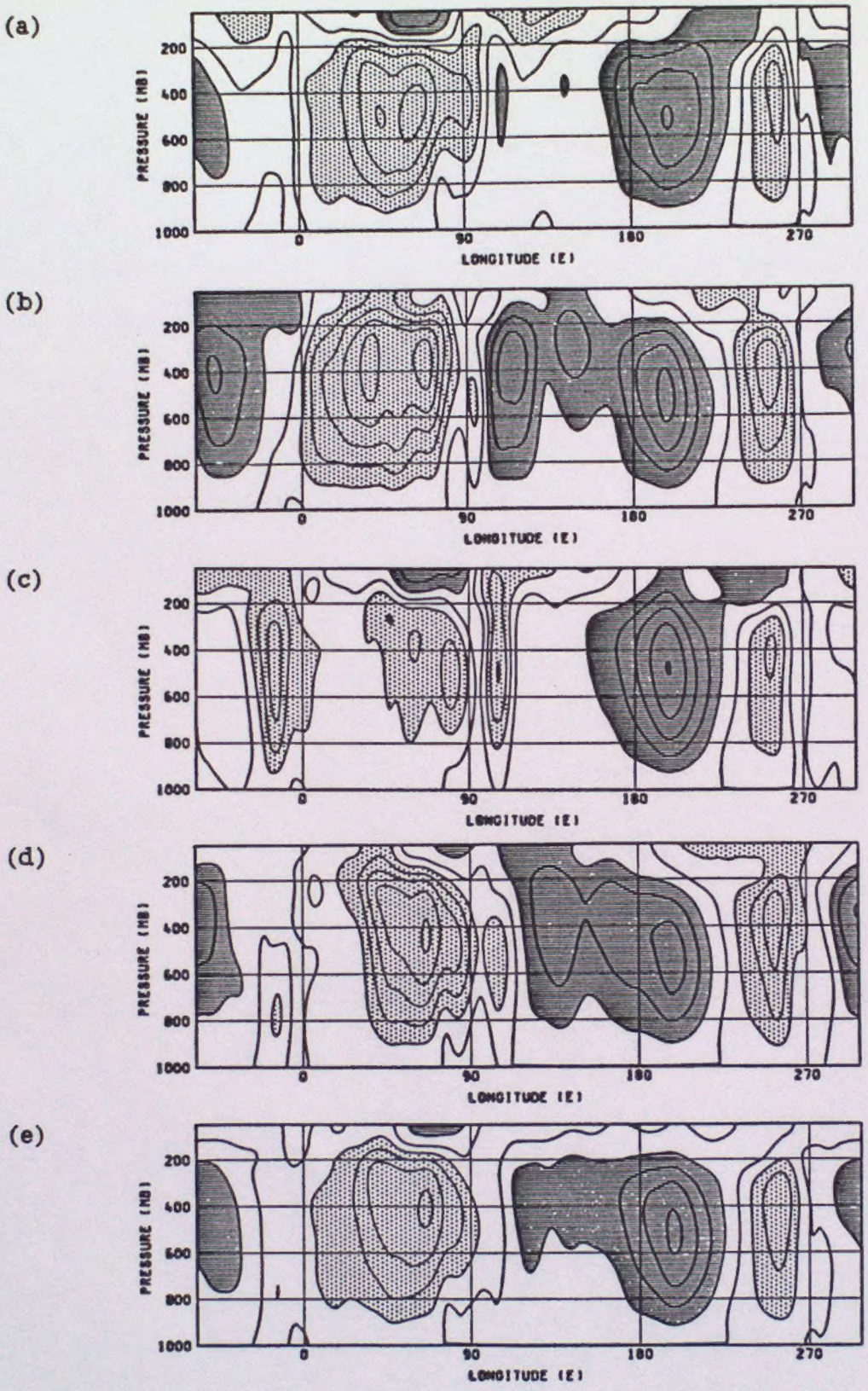

Fig.15 30-day mean (August) cross-section of the zonal divergent component of vertically integrated mass flux ($-g^{-1}\int\int vdpdy$) between 6°N and 24°N at (a) 0600, (b) 1200, (c) 1800, (d) 2400 GMT, and (e) mean of all 6-hourly data. Contour interval is 4×10^9 kgs^{-1}, with values greater than 4×10^9 stippled, and values less than -4×10^9 hatched. Flow is clockwise around hatched areas.

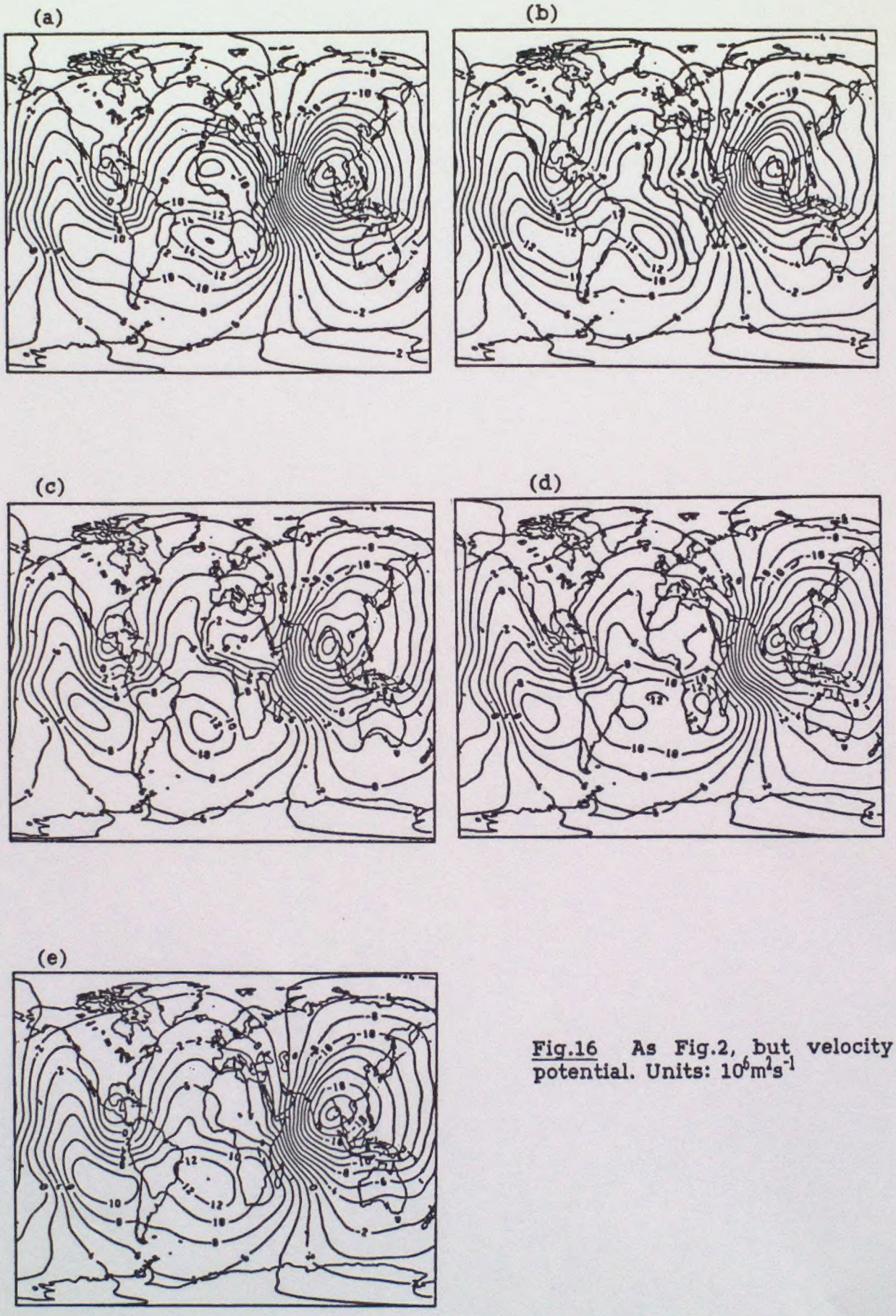

Fig.16 As Fig.2, but velocity potential. Units: $10^6 m^2 s^{-1}$